

Supporting Information to

Electrochemiluminescence Imaging of Cellular Contact Guidance on Microfabricated Substrates

Lurong Ding, Ping Zhou*, Yajuan Yan, Bin Su*

Key Laboratory of Excited-State Materials of Zhejiang Province, Department of
Chemistry, Zhejiang University, Hangzhou 310000, China

Email: subin@zju.edu.cn

Table of Contents

Figure S1. BF and ECL Images of A549 Cells on Different Electrodes

Figure S2. The Area of PC12 Cells Quantified from ECL Images

Figure S3. Quantitative Analysis of A549 Cells on Different Electrodes

Figure S4. Imaging Collective Cell Migration right after Scratch

Figure S5. Imaging Collective Cell Migration 2 h after Scratch

Figure S6. Imaging Collective Cell Migration 8 h after Scratch

Figure S7. Imaging Collective Cell Migration 12 h after Scratch

Figure S8. Imaging Collective Cell Migration 24 h after Scratch

Figure S9. Quantification of the Percentage of Cells Having Preferential Orientations
towards the Scratch at Different Time Intervals

Figure S10. Morphological Change of Cells under Drug Treatment

Figure S11. Collective Cell Migration on Flat Electrodes with Drug Treatment

Figure S12. Collective Cell Migration under the Perpendicular Condition with Drug
Treatment

Figure S13. Collective Cell Migration under the Parallel Condition with Drug
Treatment

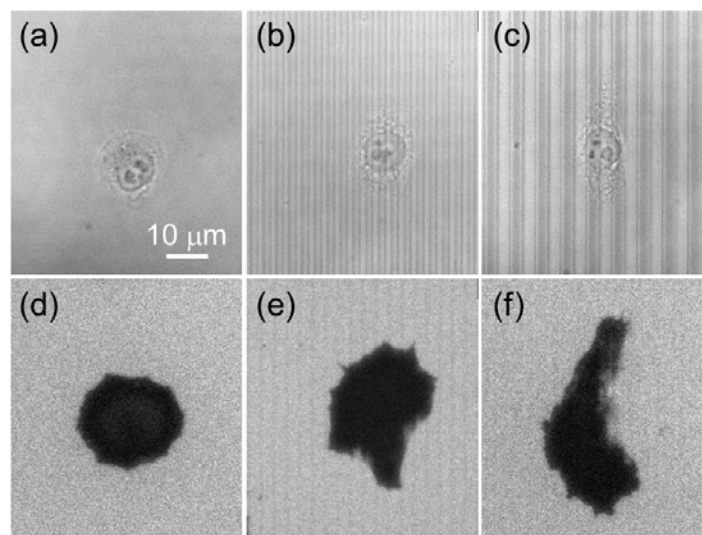


Figure S1. BF (a-c) and corresponding ECL images (d-f) of A549 cells on the surfaces of flat (a, d), MG3 (b, e), MG6 (c, f) electrodes. The scale bar is 10 μm . ECL images were recorded in 0.01 M PBS (pH 7.4) containing 100 μM $\text{Ru}(\text{bpy})_3^{2+}$ as luminophore and 25 mM HEPES as coreactant. A constant voltage of +1.3 V (vs. Ag/AgCl) was applied.

Figure S1 compares the morphology of A549 cells on flat, MG3, MG6 electrodes. When comparing BF and corresponding ECL images, it is hard to distinguish the periphery of cells in BF images (**Figure S1a-c**), while that in ECL images is easily recognized (**Figure S1d-f**). The contrast of BF images is not good enough to recognize between electrode and cell, because the periphery of cell is generally very thin. However, thanks to its advantage of surface sensitivity, ECL imaging can reveal the cell periphery. It can be seen that A549 cells on flat electrodes display a round shape (**Figure S1d**). Cells on micro-grooved electrodes show a bipolar appearance and are obviously elongated. Cells also orient apparently along the grooves on both MG3 and MG6 electrodes. Besides, there are some protrusions observed along the grooves (**Figure S1e-f**).

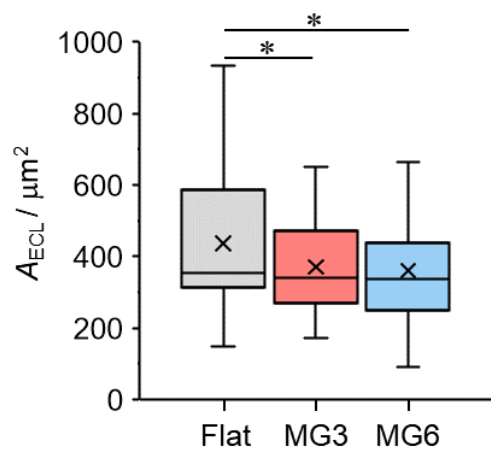


Figure S2. The ECL area of PC12 cells on flat, MG3 and MG6 electrodes. (*) $p < 0.05$.

Figure S2 shows the ECL area (A_{ECL}) of cells cultured on flat, MG3 and MG6 electrodes, respectively. A_{ECL} of cells on micro-grooved electrodes are smaller than that of cells on flat electrodes, because the grooves restrict the spreading of cells.

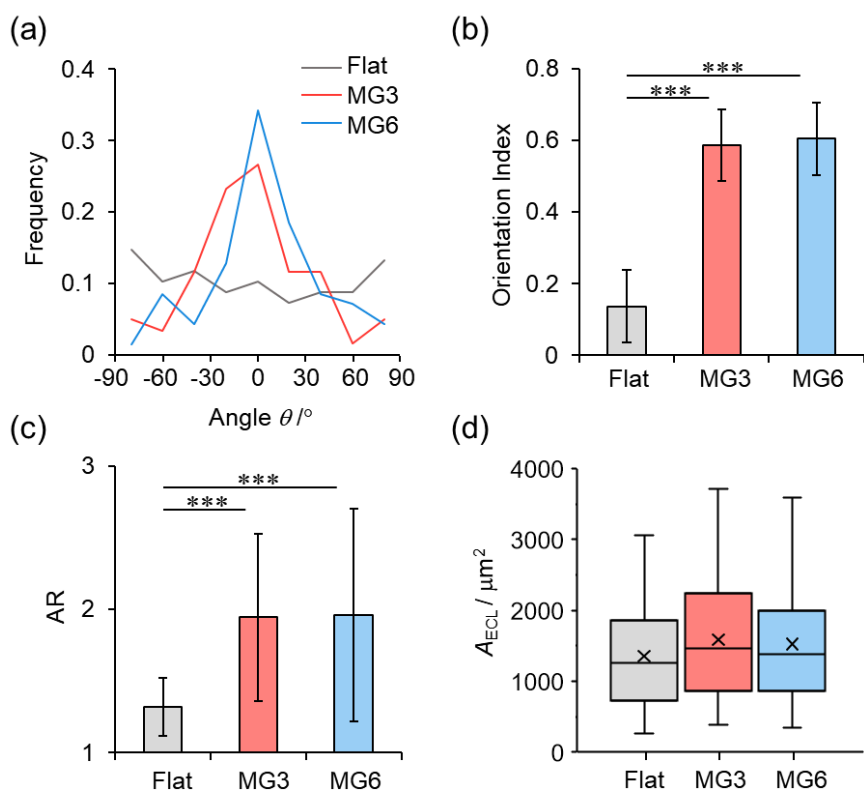


Figure S3. The distribution of orientation angle (a), orientation index (b), AR (c) and ECL area (d) of A549 cells on flat, MG3 and MG6 electrodes. (*) $p < 0.05$; (***) $p < 0.001$.

As shown in **Figure S3a**, A549 cells on flat electrodes display a random distribution. The orientation angles of A549 cells on MG3 electrodes distribute mainly between -45° and $+45^\circ$, while those on MG6 electrodes mainly between -30° and $+30^\circ$, meaning that the distribution of angles of A549 cells on MG6 electrodes is more concentrated. It is also confirmed by the orientation index, as shown in **Figure S3b**. The average of orientation index of cells on the flat electrodes is only 0.14. Meanwhile, that for cells on MG3 and MG6 electrodes is 0.58 and 0.60, respectively. The index of cells on MG6 electrodes is slightly higher than that on MG3 electrodes. The aspect ratio (AR) of cells is also compared to elucidate the morphology of A549 cells (**Figure S3c**), which is 1.32, 1.94 and 1.95 in average for cells on flat, MG3 and MG6 electrodes, respectively, indicating that cells on micro-grooved electrodes adopt a more elongated morphology. There is no significant difference of A_{ECL} between cells on flat and micro-grooved electrodes.

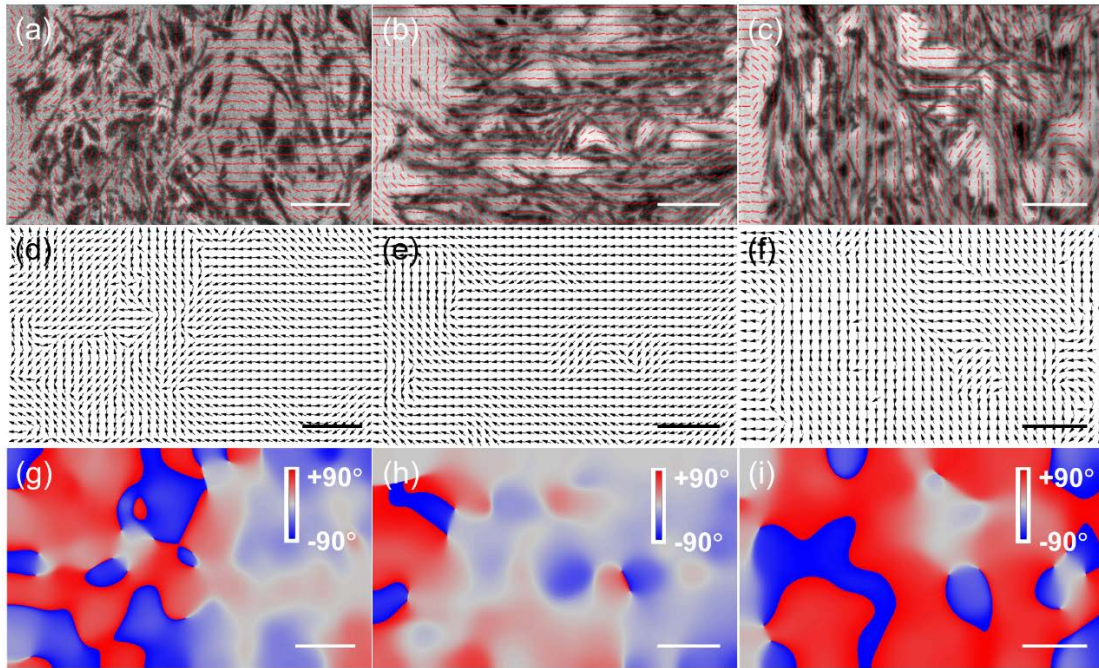


Figure S4. ECL (a-c) images of a monolayer of PC12 cells captured right after scratch. Red short lines overlaid in ECL images show the local orientations of cells, which are also shown as black arrows (d-f) and color codes graphs (g-i). The images in the left panel (a, d, g) are obtained on flat electrodes, those in the middle (b, e, h) represent the case where the orientation of wound is perpendicular to grooves, while those in the right (c, f, i) stand for the condition in which the orientation of wound is parallel to grooves. The sequence is the same in the following Figure S5-S8, unless otherwise stated. The scale bar in all graphs is 50 μm .

As observed in **Figure S4**, right after scratch, cell-matrix adhesions of cells grown on the flat electrode distribute randomly without preferential direction, adhesions of cells under perpendicular condition align alongside the grooves, and the orientations of cell-matrix adhesions of cells under parallel condition are perpendicular to the grooves. That is to say, at the very beginning of migration, the orientations of cell-matrix adhesions are solely under the influence of topographic cues.

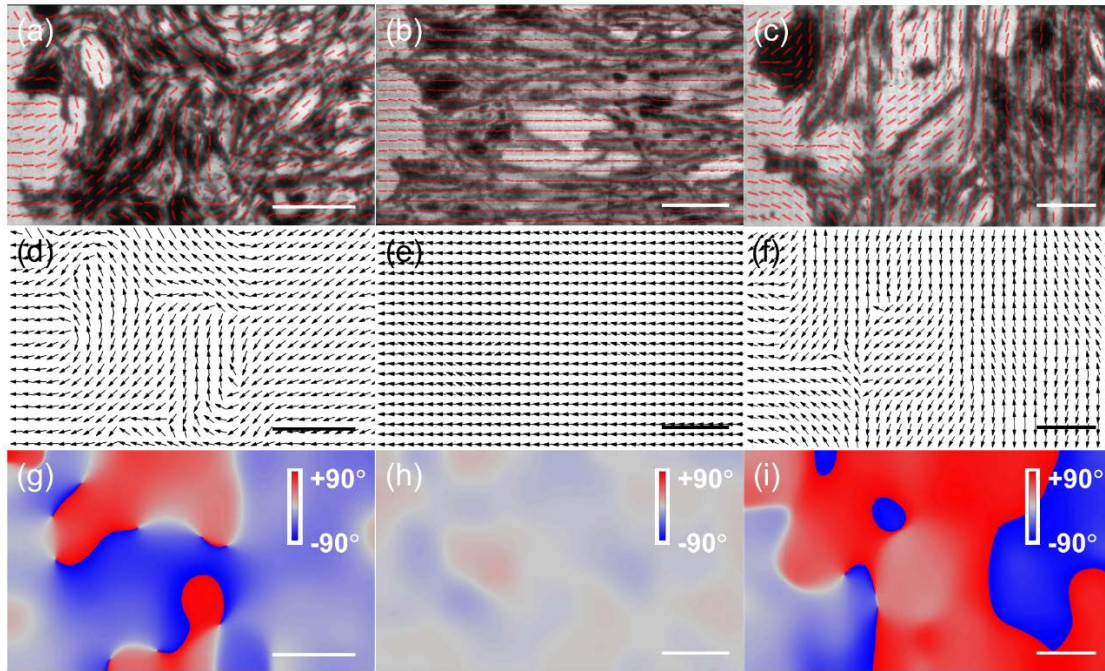


Figure S5. All conditions are the same as that in Figure S4, except that the pictures were captured after migration for 2 h.

As shown in Figure S5, after 2h, cells on flat electrodes have already adjusted the orientations of cell-matrix adhesions and started to migrate towards the wound, as the orientation of leading cells turned perpendicular to the wound. The grooves facilitate the collective cell migration of cells under the perpendicular condition, so cells move along the grooves and do not have to adjust orientations. However, cells under the parallel condition are hindered by the grooves. Only cells in the vicinity of the wound change their direction, while the rest are still parallel to the wound.

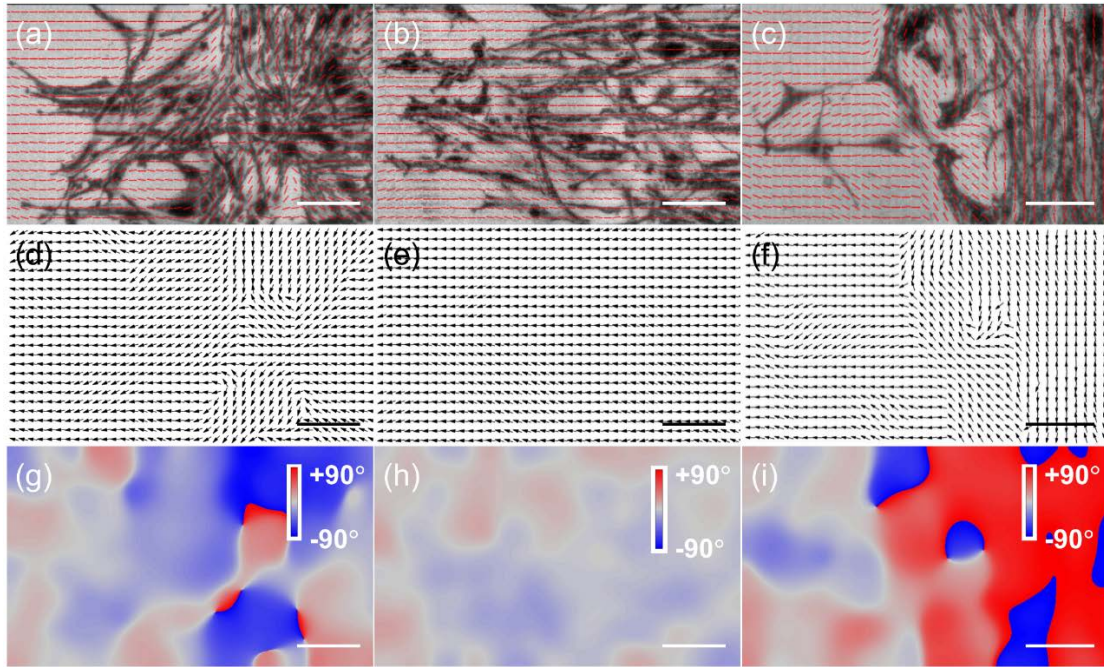


Figure S6. All conditions are the same as that in Figure S4, except that the pictures were captured after migration for 8 h.

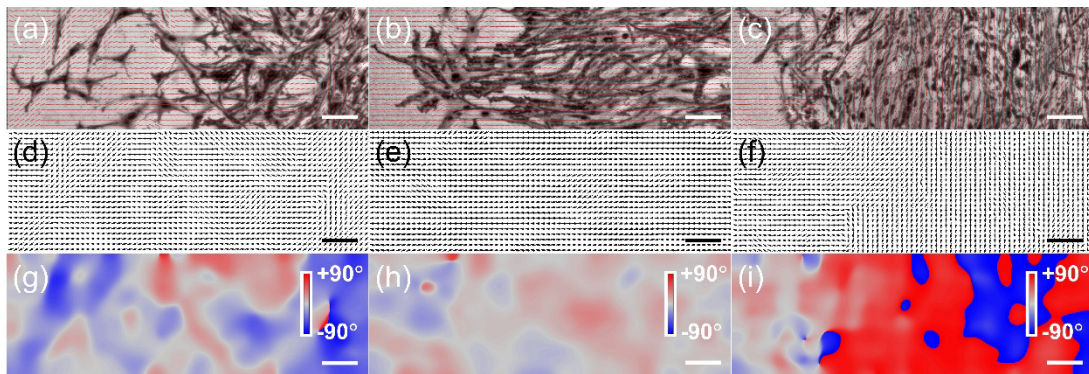


Figure S7. All conditions are the same as that in Figure S4, except that the pictures were captured after migration for 12 h.

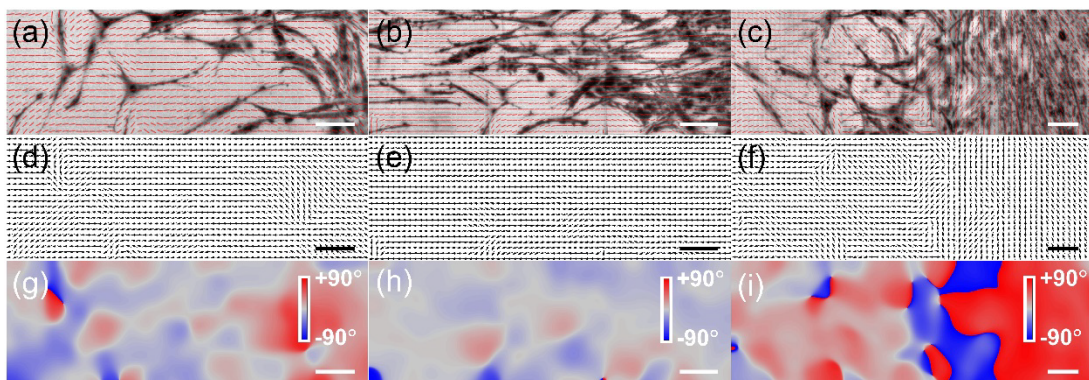


Figure S8. All conditions are the same as that in Figure S4, except that the pictures were captured after migration for 24 h.

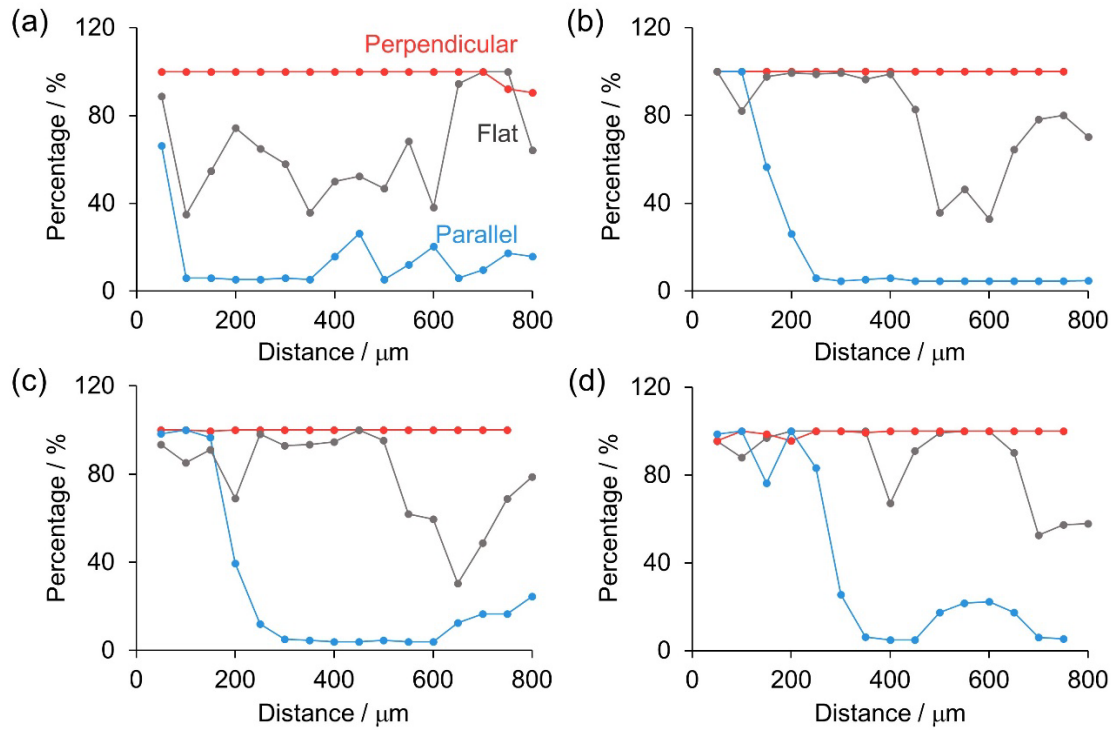


Figure S9. Quantification of the percentage of cells that have preferential orientations towards the scratch as a function of distance from the leading edge of cell sheet after migration for 2 h (a), 8 h (b), 12 h (c), 24 h(d).

As time goes by, the region of cells that have adjusted their orientation is gradually expanding. And at different migration time intervals, the region of cells on different electrodes follows an order of perpendicular condition > flat electrodes > parallel condition.

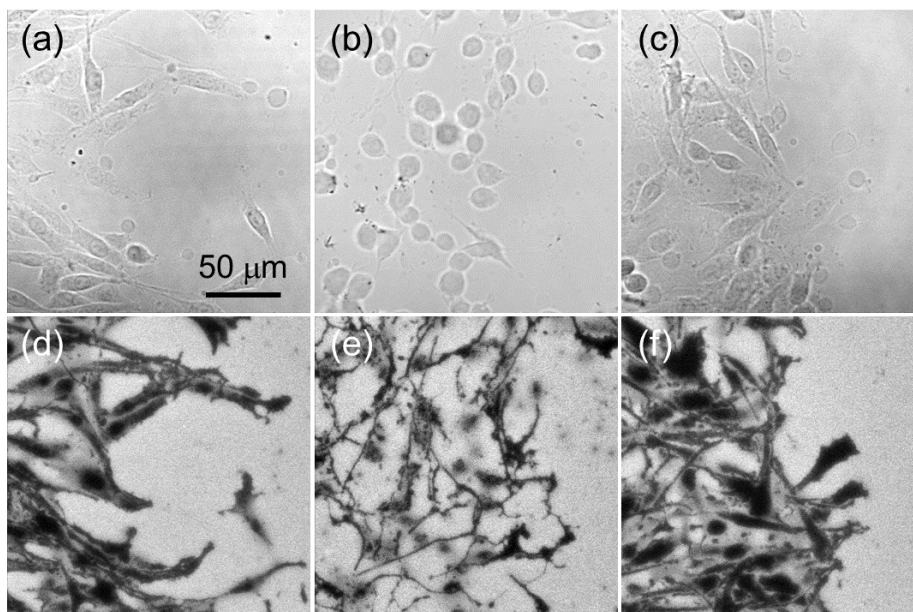


Figure S10. BF (a-c) and corresponding ECL (d-f) images of PC12 cells in the absence (a, d) and presence of blebbistatin (b, e) or RGD (c, f). The scale bar is 50 μm.

Figure S10 compares the morphology of cells under blebbistatin or RGD treatment. After 4 h of blebbistatin treatment, the morphology of PC12 cells changed a lot and turned into a dendritic-like shape. There is no obvious difference of cell morphology between cells with or without RGD treatment.

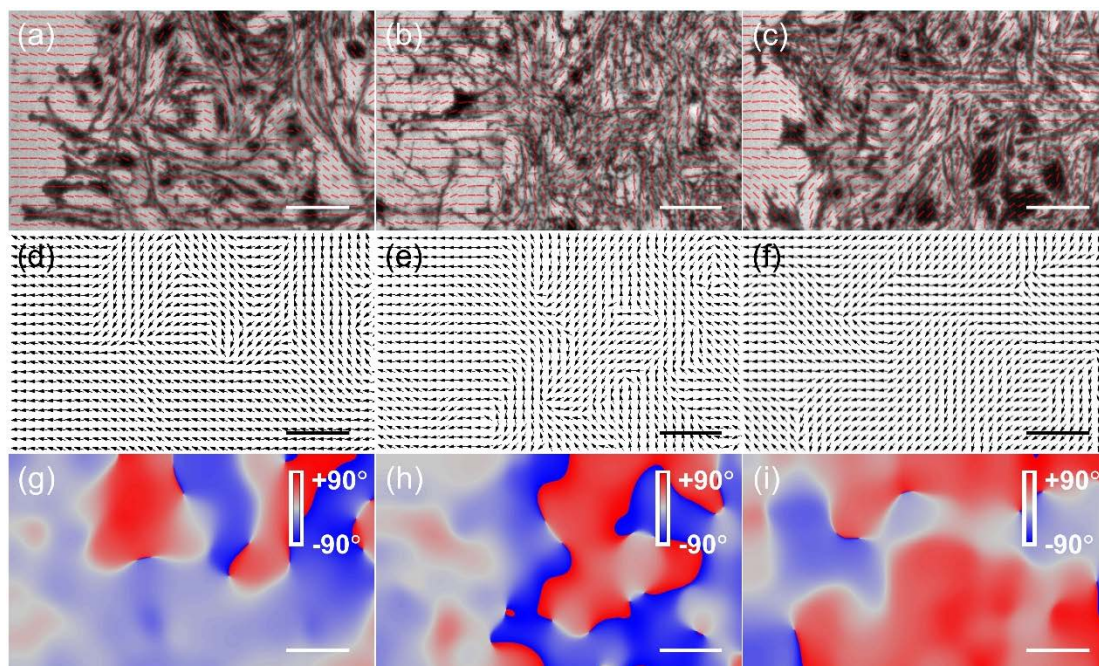


Figure S11. ECL (a-c) images of a monolayer of PC12 cells on the flat electrode captured at 4 h after migration under drug treatment. Red short lines overlaid in ECL images show the local orientations of cells, which are also shown as black arrows (d-f) and color-coded graphs (g-i). The images in the left panel (a, d, g) were obtained with the control group without drug treatment, those in the middle panel (b, e, h) were obtained for cells under blebbistatin treatment, and those in the right panel (c, f, i) were captured for cells under RGD treatment. The sequence is the same for the following Figures S12 and S13, unless otherwise stated. The scale bar in all graphs is 50 μm .

The speed of cells changing their orientations towards the wound was slowed down in the presence of blebbistatin or RGD, as the distance that cells have adjusted direction was decreased.

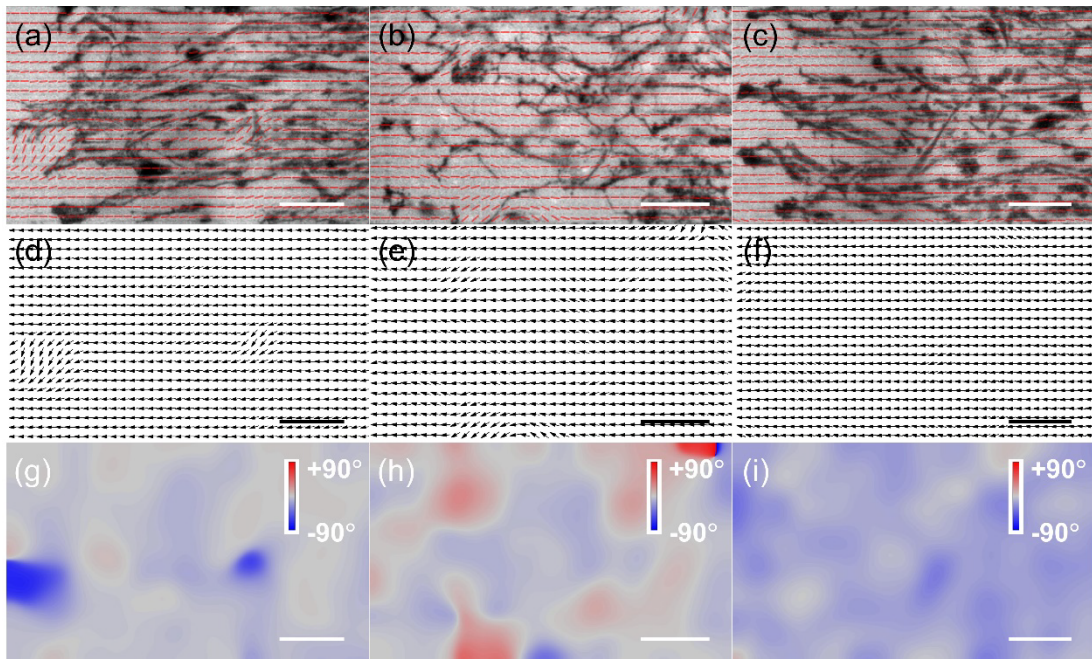


Figure S12. All conditions are the same as that in Figure S9, except that cells were cultured on micro-grooved electrodes and the directions of grooves are perpendicular to the wound.

Blebbistatin or RGD allows cells under the perpendicular condition to align along the micro-grooves.

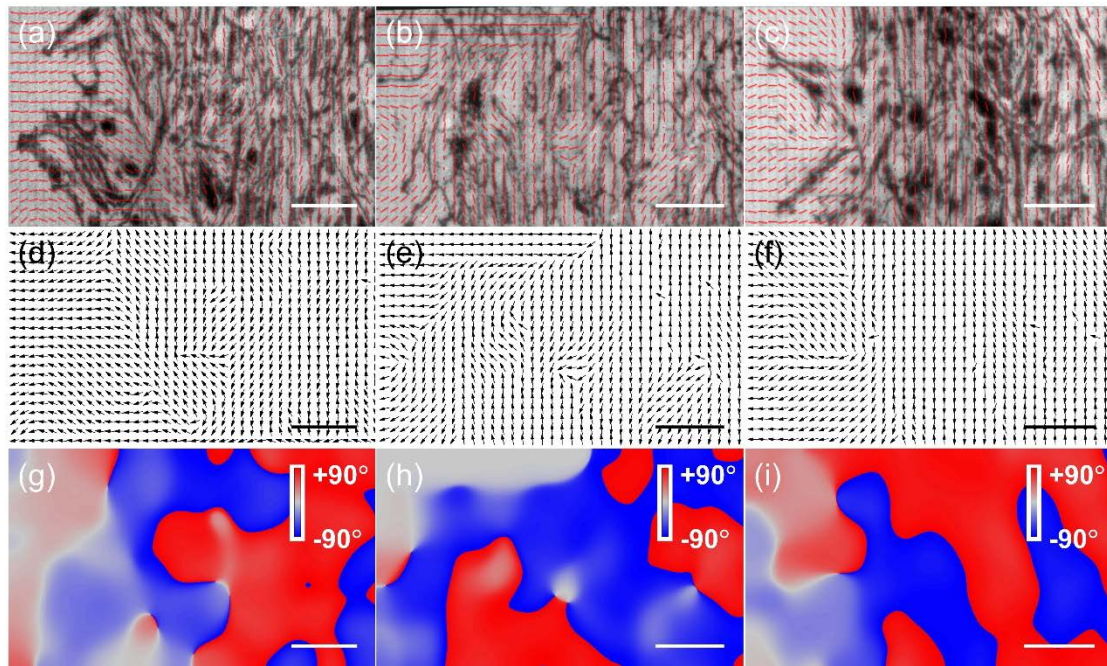


Figure S13. All conditions are the same as that in Figure S9, except that cells were cultured on micro-grooved electrodes and the directions of grooves are parallel to wound.

Similar to the group that cells on flat electrodes, the speed and the region of cells changing their orientation towards the wound were also diminished in the presence of blebbistatin or RGD.